Railway catenary tension force monitoring via the analysis of wave propagation in cables

Stefano Derosa[a]*, Petter Nåvik[a], Andrea Collina[b], Anders Rønnquist[a]

[a]Norwegian University of Science and Technology, Department of Structural Engineering, Rich. Birkelandsvei 1A, 7491 Trondheim, Norway

[b]Politecnico di Milano, Department of Mechanical Engineering, Via La Masa 34, 20158 Milano, Italy

*Corresponding author

Authors' E-mail addresses:

- Stefano Derosa: stefano.derosa@ntnu.no
- Petter Nåvik: petter.r.navik@ntnu.no
- Andrea Collina: andrea.collina@polimi.it
- Anders Rønnquist: anders.ronnquist@ntnu.no

Abstract

The tensioning forces applied to the contact wire in a railway catenary system influence the performance of the line. In this paper, a method to monitor the status of such tensioning forces is proposed based on the dependency that the waves that propagate through a tensioned wire have on the forces that pull the wire itself. A novel analytical formulation for the propagation of waves in a tensioned wire was proposed, and it was used to obtain the vertical acceleration of the wire when an external force acts as a concentrated input. The analysis of the acceleration with a moving standard deviation allowed a method to be defined for the generation of an index that describes the trend of the tensioning forces. The method was then tested on the wire accelerations obtained with laboratory tests and, afterwards, on the accelerations recorded on a contact wire of an electric railway regularly in operation and excited with the same kind of input.

Keywords: railway catenary systems, structural health monitoring, wave propagation, cable systems dynamics, structural dynamics

1. Introduction

For electric railways, a fundamental part of the infrastructure are the catenaries. These systems are essentially a flexible structure built with cables tensioned at both ends with concrete weights. A peculiar characteristic of catenary systems is that they have a variable stiffness along the structure and very low damping. Trains collect the electricity from catenaries thanks to a roof mounted mechanism called pantograph.

The importance of understanding the dynamic behaviour of the coupled pantograph-catenary system has been well known since the first studies conducted by Gostling et al.[1], both for new and existing infrastructures. Since then, many aspects of the system dynamics have been studied, as can been seen in the review on the topic by Bruni et al.[2].

One of the main branches of the research focuses on the development of numerical models for the representation of the pantograph-catenary interaction dynamics[3]. These models are used to perform dynamic assessments of the existing infrastructure (with finite elements[4] or analytically[5]), optimize existing[6] and new[7] infrastructure designs, evaluate system damping either from accelerations[8] or from displacements[9], and test for higher speed both purely numerically[10] or with hybrid models[11], avoiding the need to physically reproduce the entire system[12].

An aspect related to catenary dynamics that recently started to be taken into consideration within the system modelling is the phenomenon of wave propagation along the catenary cables. The constant contact between the pantograph and contact wire creates waves in the tensioned wire system that travel ahead of the pantograph, posing a physical limit to the maximum train speed under that specific catenary configuration[13].

Due to the importance within the catenary dynamics studies, the wave propagation phenomenon has recently attracted much interest. In the literature, examples can be found on the link between wave motion and contact force[14], on applications for the wave-induced motion reduction[15] and on wave speed evaluation, either with time/frequency analysis of numerical models[16] or from the wire displacement obtained with non-contact measurements on a full-scale laboratory setup[17]. A more recent study[18] evaluated the effects of wave propagation on the vertical velocity of the wire, and a new distributed parameter model[19] and FEM model[20] able to correctly represent the wave propagation has been introduced. Wave propagation has also been employed as a monitoring tool in railways, even though not explicitly on railway catenaries. Examples can be found for the long-term evaluation of rail modes of vibrations[21] or for the detection of defects on the rail surface[22].

The objective of this paper is to use the wave propagation for the structural health monitoring of the railway catenaries. In particular, the investigation is focused on the behaviour of the tensioning forces applied to the contact wire, which are an important parameter for defining the performance of the system. The analysis is based on the evaluation of the moving standard deviation of the contact wire

vertical accelerations. The influence that the wire tensioning forces have on the wave propagation was first investigated on the wire vertical accelerations obtained with a novel analytical formulation for the propagation of waves in a tensioned wire. Afterwards, the same process was applied to the vertical accelerations measured during laboratory tests and field measurements. Given the importance of the contact wire acceleration for the whole process, section 2 explains the characteristics of accelerations of the railway catenaries in more detail. Section 3 is dedicated to the novel analytical formulation for the wave propagation in a tensioned wire and explains how the accelerations used to build the method were evaluated. Due to the need to validate the method on real data, laboratory tests were performed in a controlled environment and explained in section 4. The last step was to retrieve acceleration data from the field, as shown in section 5, to also apply the method on data coming from a contact wire in regular service. For both laboratory tests and field measurements, a wireless measurement system[23] was used. This allowed data to be obtained that were easy to collect, making the method feasible for large infrastructure monitoring applications. With a such wireless system, in fact, the need for supplementary structures (as in Diana et al.[24] and Drugge et al.[25]) or for service interruption[26] is minimized.

The method used to process the data is explained step by step in section 6, and the results from the analysis performed on the analytical formulation, laboratory tests and field measurements are all gathered and discussed in section 7. Finally, conclusions are drawn in section 8.

2. System Acceleration

When excited by an external input, typically a passing train or even the wind, the catenary system features motions in both vertical and lateral directions due to its flexible nature and low damping. For the dynamic assessment, both the vertical and lateral directions are used. However, in this study only the vertical accelerations are taken into account because of the nature of the considered phenomenon. The waves generated by the pantograph passage travel along the longitudinal direction and generate displacement and acceleration only in the vertical plane[13]. This chapter then focuses on how a catenary system works in the vertical direction when specifically excited by the passage of a train.

Several measurement campaigns have been conducted on the Norwegian Railway Network in the past year with the aforementioned wireless systems, which can record accelerations in three directions on both the contact and messenger wires[23]. Figure 1 shows a vertical acceleration signal recorded on a Norwegian Railway contact wire during a train passage. Such a signal can be divided into four main parts, each representing a different contribution of the train to the catenary system dynamics[8]:

1. Environmental excitation, where the recorded accelerations are mainly associated with effects not linked to the approaching train (mostly wind, but potentially ground vibrations from the train or other sources around the sensor location);

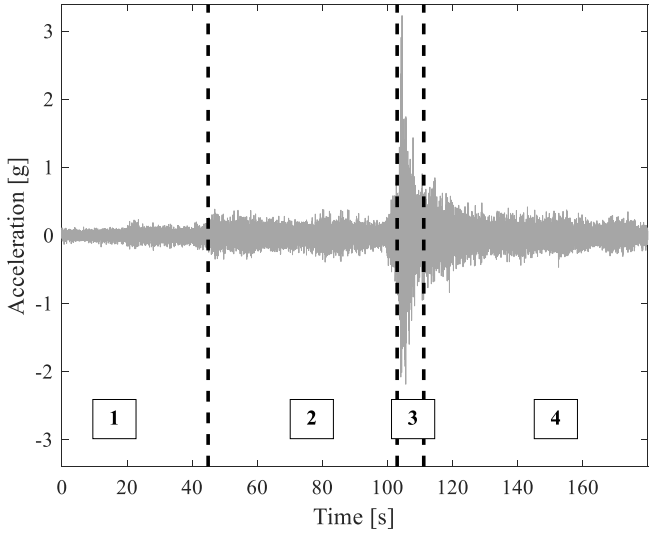

Figure 1: Contact wire vertical acceleration during train passage.

2. Pre-passage, when the level of the signal starts to increase due to the arrival of waves that propagate from the contact point between the pantograph and catenary wires up to the sensor position;
3. Train passage, where the acceleration has a peak associated with the passage of the pantograph at sensor locations; and
4. Post-passage, where the system dynamics is generally dominated by free decay behaviour.

The fourth part is well suited for dynamic assessments of the catenary system and damping identification. The second part, on the other hand, provides insights regarding the phenomenon of wave propagation in a dispersive mean. The origin of these waves can be traced back to the catenary design. Although the goal is to achieve a constant stiffness along the entire contact wire, the presence of concentrated masses such as droppers and steady arm clamps introduces points of high stiffness. When the pantograph collector encounters one of these points, the effect on the contact wire is the same as an impulse load at the clamp position. As a result, each time the train passes a dropper or a steady arm a wave is generated and propagates along the contact wire, droppers and messenger wire. Furthermore, every time a wave encounters a clamp or arrives at the section end, a reflected wave is generated that travels backward in the opposite direction. Propagation between neighbouring sections is not possible due to the mechanical separation between wires. The signal portion included in section 2 of Figure 1 is the sum of all the waves generated within the instrumented catenary section. The amount of waves recorded by the accelerometer makes it difficult to extract the shape of a single wave from field measurements. Consequently, analysis on a simpler setup was preferred. For the laboratory tests, the setup consisted of a single tensioned contact wire excited with a single hit by a modal hammer. For the field measurement the same setup was reproduced on a contact wire mounted on a side track section, and the excitation was of the same type as per laboratory tests. The separation from the operating line ensured the absence of influence from trains regularly running on the line.

3. Analytical Formulation of Wave Propagation

The analytical formulation that represents the dynamics of the system is presented together with the assumptions considered for this case. In the literature, analytical formulations have been proposed for similar types of problems based on both string models (Metrikine et al.[27]) and beam models (Dahlberg[28]). What they all have in common is excitation by a moving force, which does not represent the same case study as in this work. A later work by Cho[29] proposed the use of the same formulation as given by Dahlberg but with the speed of the moving force equal to zero. In the present paper, a different approach is selected by using modal analysis to obtain a complete solution for the wave propagation caused by an impulse. The main advantage of this procedure, which already found application in pantograph-catenary interaction dynamics studies as Facchinetti et al.[30] and Gregori et al.[31], is that it can be applied to model a load concentrated in both time and space in a relatively simple way, as done by Rønnquist[32]. Furthermore, it is possible to include a specific number of modes, allowing, among other things, the matching of the frequencies of given terms for comparison. Specifically, in this work, the comparison was needed with the signals recorded in the laboratory test and in the field measurements, which are naturally limited by the sampling frequency.

3.1. Modal parameters

Assuming that the n^{th} mode shape $\phi_n(x)$ of the system is sinusoidal with the following equation:

$$\phi_n(x) = \sin\frac{n\pi x}{L} \tag{1}$$

and that the corresponding time-dependent function is $\eta_n(t)$, the displacement response can be written as follows:

$$r(x,t) = \sum_{n=1}^{N} \phi_n(x)\eta_n(t) \tag{2}$$

Concerning the acceleration response, the equation is the same, except for the time-dependent function, which is differentiated twice with respect to time.

$$\ddot{r}(x,t) = \sum_{n=1}^{N} \phi_n(x)\ddot{\eta}_n(t) \tag{3}$$

To solve the equation of motion with the mode superposition method and obtain the values of η_n and $\ddot{\eta}_n$, the modal structural properties, such as the mass and load, must be evaluated as follows:

$$\widetilde{M}_n = \int_L m(x)\phi_n^2(x)dx \tag{4}$$

$$\tilde{p}_n(t) = \sum_i P(x_i,t)\phi_n(x_i) \tag{5}$$

where $m(x)$ is the linear mass of the wire and $P(x_i,t)$ represents the concentrated loads at time t and location x_i on the wire. In this case, the force is only one, and the position on the wire is x_F.

The values for the natural frequencies for a beam of length L, linear mass m_l, bending stiffness EI, axially loaded with a tension T and pinned at both ends are equal to the following:

$$\omega_n = \frac{n\pi}{L}\sqrt{\frac{T}{m_l} + \left(\frac{n\pi}{L}\right)^2 \frac{EI}{m_l}}. \tag{6}$$

Additionally, the stiffness and damping can be expressed as follows:

$$\widetilde{K}_n = \omega_n^2 \widetilde{M}_n \tag{7}$$

$$\tilde{C}_n = \zeta_n 2\omega_n \widetilde{M}_n \tag{8}$$

The values of ζ_n are evaluated using the Rayleigh formulation, choosing the parameters $\alpha = 0.062$ and $\beta = 6.13 \cdot 10^{-6}$ as in Nåvik et al. [8].

Once all modal parameters are defined, the equation of motion of an arbitrary mode n can be expressed as follows:

$$\ddot{\eta}_n(t) + 2\zeta_n\omega_n\dot{\eta}_n(t) + \omega_n^2\eta_n(t) = \frac{\tilde{p}_n(t)}{\widetilde{M}_n} \tag{9}$$

In addition, a solution for short impulse loads with duration $\Delta\tau$ can be found. For such a case, the displacements at $\Delta\tau$ are equal to zero, and the speed is the ratio between the impulse and the modal mass ($\dot{\eta}_n(\Delta\tau) = I_n/\widetilde{M}_n$). The impulse value is readily obtainable from the following equation:

$$I_n = \int_0^{\Delta\tau} \tilde{p}_n(t)dt \tag{10}$$

The latter consideration is important in the definition of the initial conditions for displacement and speed to determine the impulse response function of the system, namely, the solution needed for this problem:

$$\eta_n(t) = h(t) = \frac{I_n}{\widetilde{M}_n\omega_d}\sin(\omega_d t)\, e^{-\zeta_n\omega_n t} \tag{11}$$

where $\omega_d = \omega_n\sqrt{1-\zeta_n^2}$ is the damped natural frequency.

3.2. Modal load

According to Eq. (10), the impulse is evaluated as the time integral of the modal force function, which is the product of the actual force and the mode shapes, as shown in Eq. (5). In this case, the force function $P(x_F, t)$ used is that obtained via the impulse tests performed in the laboratory on the wire itself. An average among all the force signals recorded during the tests with the $100\,mm^2$ wire

provided the needed function. Furthermore, a sensitivity analysis on the time integral over said function allowed the time window for the impulse value computation to be chosen.

3.3. Solution

By using the Duhamel integral for the solution evaluation, the input force can be divided into short impulses (in this case, the duration is equal to $5 \cdot 10^{-4}\ s$) and each of them can be integrated over the time interval analysed, including both the transient and steady state parts of the response. In this way, the system response can be formulated as follows:

$$\eta_n(t) = \left(\eta_{t_0} \cos \omega_d (t - t_0) + \frac{\dot{\eta}_{t_0} + \eta_{t_0} \zeta_n \omega_n}{\omega_d} \sin \omega_d (t - t_0)\right) e^{-\zeta_n \omega_n (t - t_0)} + \\ + \frac{1}{\widetilde{M}_n \omega_d} \int_{t_0}^{t} \tilde{p}_n \sin\left(\omega_d (t - \tau)\right) e^{-\zeta_n \omega_n (t - \tau)} \tag{12}$$

where the first term takes into account the vibrations already present in the system and the second term accounts for the new contribution from the subsequent short impulse. The input force curve is divided into short impulses because the duration was not infinitesimal, and if the entire energy signal was concentrated in a single impulse, the result would be wrong, both in terms of the shape and magnitude of the response time history. With the equation obtained, the acceleration response was evaluated with the same parameters as used both in the laboratory tests and on field measurements. The response was then extracted at the corresponding sensor positions.

4. Tensioned Wire Laboratory Test

A simplified setup for a laboratory test was selected to test the behaviour of the propagating waves in a controlled environment before field measurements. A copper/silver contact wire with a $100\,mm^2$ section (type AC-100 according to [33]) was fastened with pin joints at both ends to a long-stroke pulling machine. The assigned displacement ensured the desired mechanical tension throughout the tests. Figure 2 shows the key components of the test setup, namely, the wireless accelerometers (Figure 2a); the joints employed to secure the wire at both ends, which were also used when the wire was mounted on the catenary system (Figure 2b); and the entire wire mounted on the pulling machine (Figure 2c), with safety measures taken in case of wire failure.

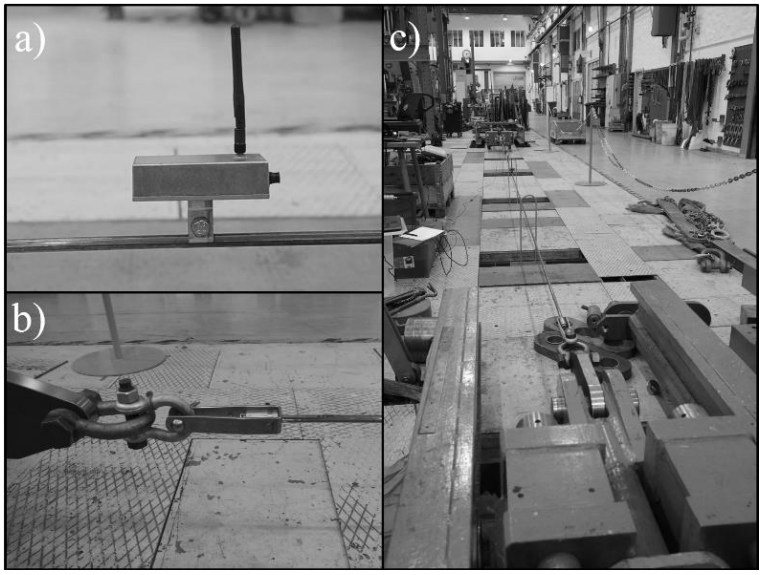

Figure 2: Laboratory set-up: a) accelerometer, b) pin joint, and c) wire.

Figure 3 provides details of the test configuration. For the $100\,mm^2$ wire (named CW100), the measured length was $10.095\,m$, and the sensors were placed at distances of $d_{S1/A} = 4.591\,m$ for

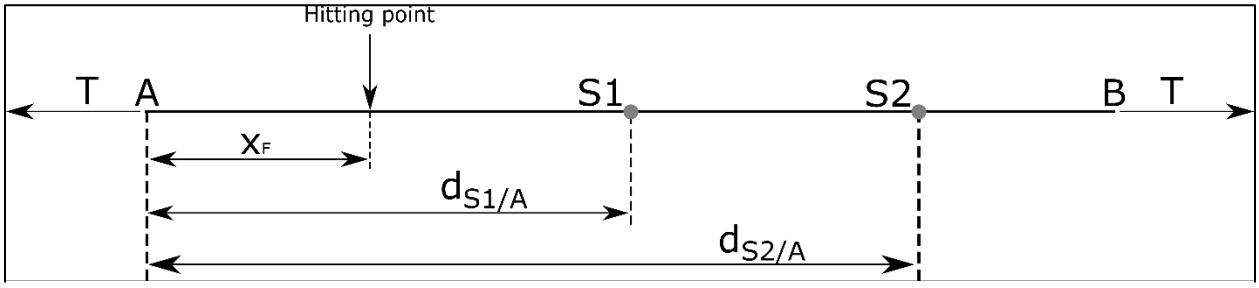

Figure 3: Laboratory set-up. Distances are from reference end A at the left side of the figure.

sensor S1 and $d_{S2/A} = 7.085\ m$ for sensor S2. All the distances were evaluated with a laser from reference end A. Tension values of $10\ kN$ and $7.06\ kN$ were applied to the wire during the test sessions. These values are typical tensions for this type of wire in operation. Several vertical accelerations were recorded with a sampling frequency $f_s = 200\ Hz$, each one as a result of a single hit with a modal hammer at a distance of $x_F = 2.5\ m$ from reference end A. To capture the entire acceleration signal, a pre-trigger time of 10 seconds was set for the sensors.

The intention behind the test was to see how a wave propagated along the contact wire and determine if it was possible to detect differences in behaviour when parameters such as the tension were changed.

Figure 4 shows an example of a measured signal interpolated with a cubic spline for clarity. The dispersive nature of the propagating wave can be observed. Within this signal, contributions from both the first forward wave and from the reflected ones are visible. The presence of the reflected waves is associated with the length of the wire used, which was limited by the available space between the two ends of the pulling machine. However, the wire length corresponds to the distance between two adjacent dropper clamps.

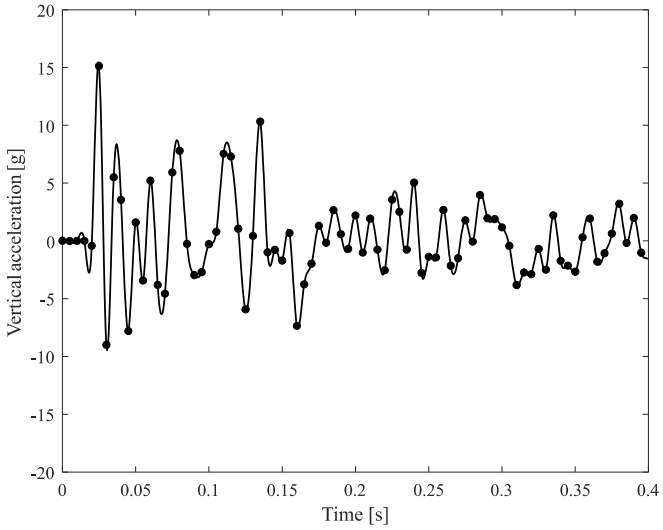

Figure 4: Vertical acceleration response of the CW100 wire with tension $T = 7.06\ kN$ at the sensor S1 location. Hit position $x_F = 2.5\ m$ from reference end A.

5. Field measurements

Field measurements were performed on one of the side tracks in place at Oppdal station along the Dovre railway line that connects Oslo and Trondheim on the Norwegian railway network. The catenary system mounted on the track is of type "Tabell 54", with a pure copper $80\ mm^2$ section contact wire. The wire length is $588\ m$ and nominal tension force is $6.93\ kN$ (Figure 5).

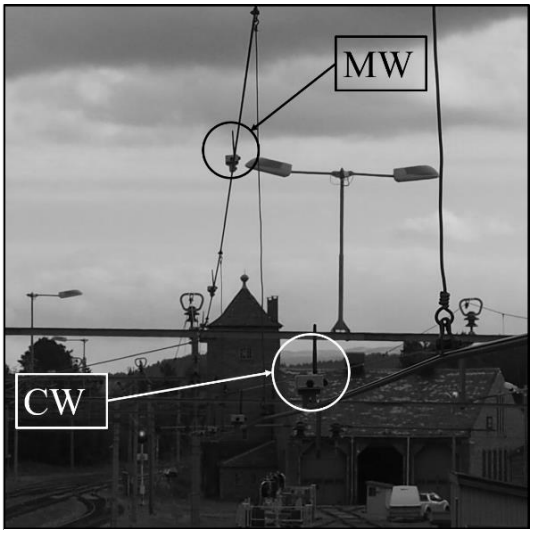

Figure 5: Field measurement set-up: sensors are mounted on contact (CW) and messenger wires (MW).

A complete set of ten sensors was installed on a single span, as per the scheme presented in Figure 6a, placing one sensor within each inter-dropper span both on the contact and messenger wires. For the scope of this work, only data from sensor number 6 were used due to its position chosen to be as close as possible to the one assigned as sensor number 1 in the laboratory tests. The comparison is then made between the full length of the cable used in the laboratory tests and the segment included between the two droppers surrounding sensor number 6 in the field measurements (Figure 6b). Distances from reference point A were $d_{S6/A} = 4.650\ m$ for sensor S6 and $x_F = 2.650\ m$ for the hitting point on the contact wire. The sensors

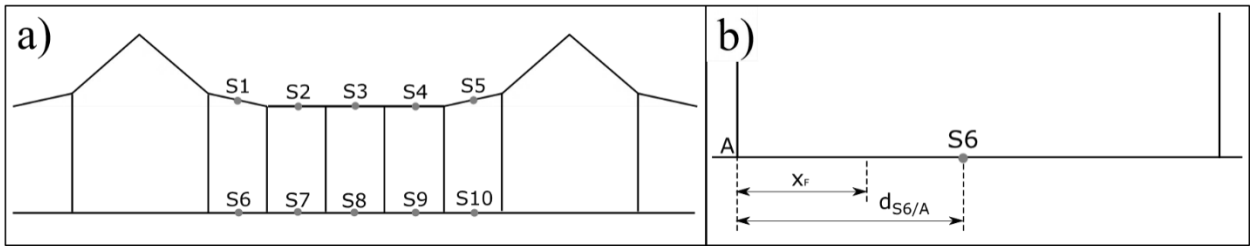

Figure 6: Field measurements set-up. Distances are from reference end A at the left side of the figure. Complete set up (a) and detail at the first sensor near the hitting point (b).

mounted during these measurements are the same as in the laboratory tests, and the type of input is again an impulse hit at a fixed distance from the sensor, with no obstacles in between them. The sampling frequency is $f_s = 200\ Hz$, and the trigger is set manually before each measurement.

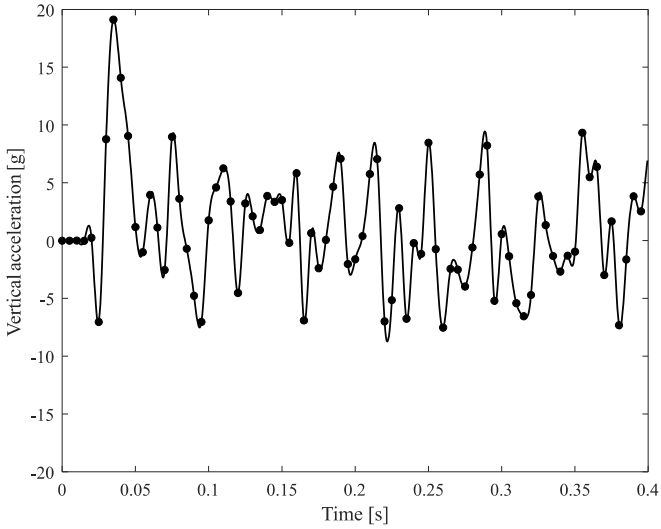

Figure 7: Vertical acceleration response of the CW080 wire with tension $T = 6.98\ kN$ at the sensor S6 location. Hit position $x_F = 2.65\ m$ from reference end A.

Figure 7 shows an example of the measured signal from sensor number 6. Also in this case, as happened with the laboratory tests, wave reflection affects the shape of the signal. In this case, however, the reflection is caused by the dropper clamps, and the coefficient is frequency-dependent. This aspect will be taken into account when simulating the signal with the analytical solution.

6. Data Processing

The method for the data processing was built on the accelerations obtained with the analytical formulation. The flexibility given by this formulation allowed the wire acceleration response to the first forwarding wave without any other disturbance to be reproduced. In addition to the characteristics of this wave, the other parameters needed for the method, such as the location of the sensor with respect to the excitation point and the analysis time window duration, were determined.

Figure 8a shows the simulated vertical acceleration of the wire when the same distance between the input force and observation point is set, but the boundaries are at an "infinite" distance. In this way, only the first wave that travels forward from the impact point to the observation point is represented. The same simulation has been repeated multiple times with different values of tensioning forces applied to the cable. It is then possible to observe how the shape of the vertical acceleration changes accordingly. Figure 8b shows, on the other hand, the dependency of the same waves on the frequency, which originates the dispersion in time. The analysis aims at taking advantage of the trend due to the tensioning forces changing in order to detect when the tension in a wire is dropping or increasing. To achieve this result, the evaluation of the signal's standard deviation is taken into account, and the

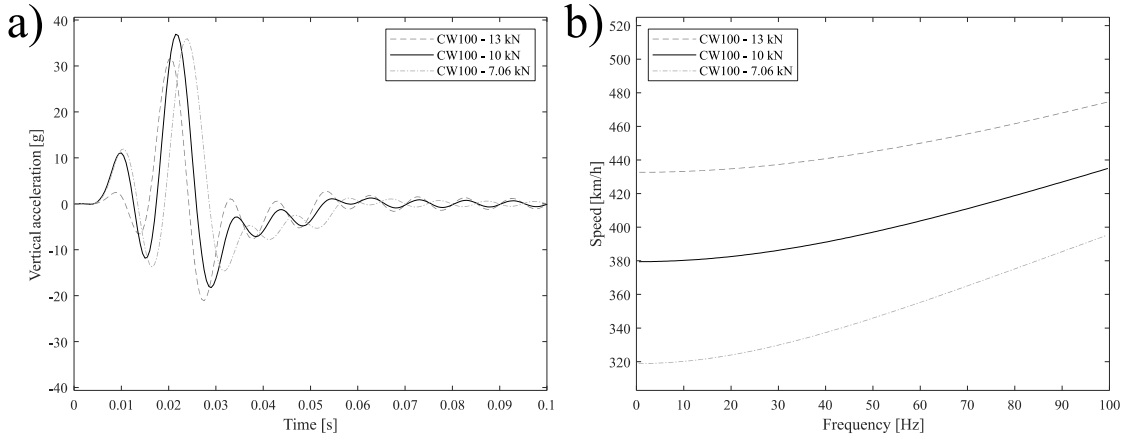

Figure 8: Simulated vertical acceleration signals (a) and respective wave propagation speed (b). The simulations have been performed with multiple tensioning force values.

comparison of its value across different wire tension settings is used as an index to spot failure in the functioning of the tensioning devices.

6.1. Sensor placement

The first step for an effective analysis is to be aware of the distance between the hitting point and the observation point. Different observation points will give different wave shapes, even when all the other parameters are kept constant. From Hayasaka[15] we can establish that a section overlap is one of the points where the pantograph gives the hardest hit to the contact wire. Since this point is known, it is possible then to choose an observation point at a set distance from it in order to define how the wave should be when the tension is the nominal value. Taking into consideration Figure 8a, it is possible to know, for example, what the wave shape would be at an observation point placed two metres from the hit (same distance as in laboratory tests and field measurements) and what would happen in the case of a shift of tension from the nominal value of $10\ kN$ to a lower or a greater one.

6.2. Analysis time window establishment

Once the observation position is settled, the duration of the first wave that travels forward from the hitting point and reaches the sensor is fixed. The index of choice for this analysis, namely, the cumulative standard deviation value, then needs to be evaluated at a determined point in order to be able to have a comparison between different catenary statuses. According to the

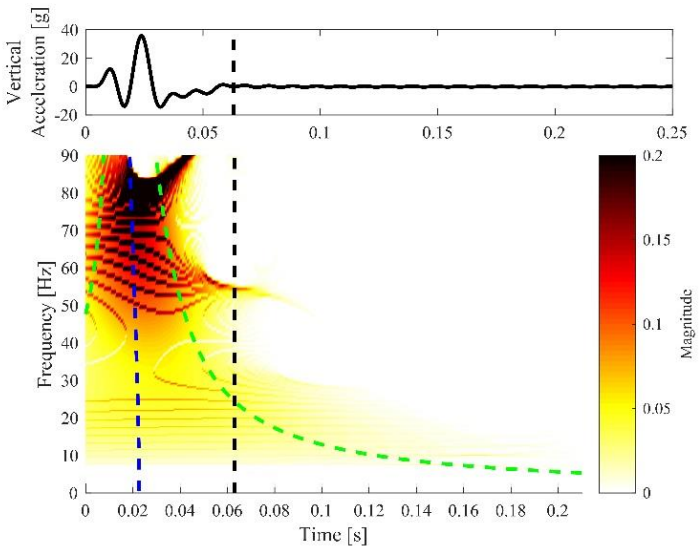

Figure 9: First forwarding wave at the observation point and relative wavelet transform. The blue line indicates the theoretical time of arrival of each frequency at the observation point. The green lines are the boundaries of the time duration of each frequency.

authors' choice, this point has been set at the end of the first wave before any reflection phenomena appear in order for the analysis to not be influenced by other components on the catenary system.

The time window duration for the evaluation of the cumulative standard deviation is set according to this choice. For this purpose, a time/frequency analysis was used, as shown in Figure 9. In the lower plot, it is easy to detect the moment in which the contribution to the wavelet transform related to the first wave drops to zero; this time instant was chosen as the end of the analysis window for the cumulative value of the moving standard deviation.

6.3. Cumulative moving standard deviation evaluation

The last step consists of the evaluation of the cumulative moving standard deviation on the recorded signal. The evaluation was performed using this parameter because of the influence that a change in tension has on it. When the wave is stretched or compressed due to a loss or increase in tension, the shape will remain the same, but every feature (positive and negative peaks) will be delayed or anticipated, bringing a change in the cumulative value of the instantaneous standard deviation accordingly. Tests on the analytical formulation showed how the difference between cases with various values of tension is detectable at the end of the first forward wave that arrives at the observation point, and the same behaviour has been reported on the measured data, both from laboratory testing and from field measurements.

7. Results

The results from the method presented in section 6 are analysed here, showing the positive outcomes in line with the idea presented at the beginning of the paper.

Figure 10a shows the results for the application of the method to the analytical formulation of the accelerations developed in section 3. The analytical formulation was evaluated with the same set-ups used in the laboratory tests (CW100 wire with $10\ kN$ and $7.06\ kN$ of tensioning force) and field measurements (CW80 with $6.98\ kN$ of tension force). Additionally, a value of $13\ kN$ of tensioning force was added for the CW100 wire. Figure 10b shows the same analysis performed on the measured data coming from laboratory tests (the two CW100 cases) and the field measurements at Oppdal station (CW080).

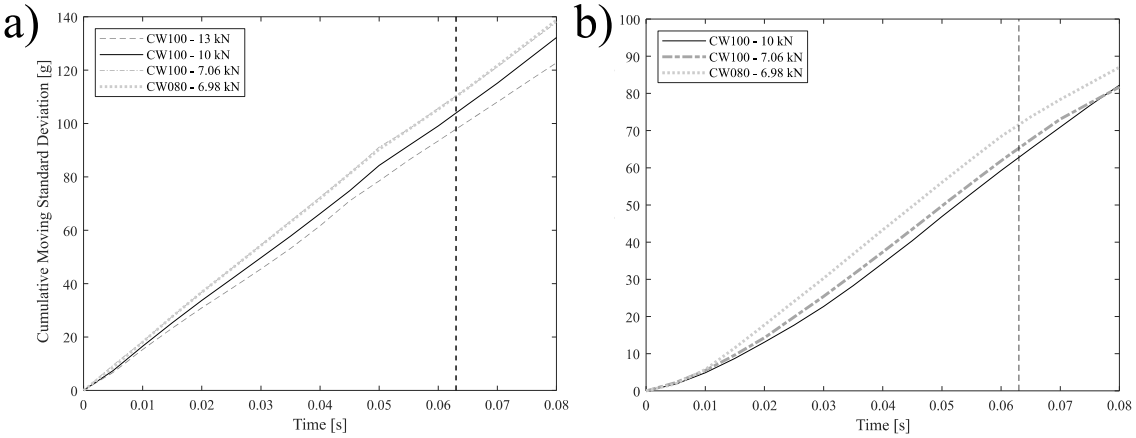

Figure 10: Cumulative moving standard deviation evaluated based on the analytical formulation (a) and on the measured signals (b) of the acceleration for different values of applied tension and contact wire cross-section. For the measured signals (b), the average values for each set-up with the corresponding characteristics are shown.

The definition of the time window in section 6.2 is used here to know at which time instant the comparison between different tensioning forces must be performed. The vertical dashed line in both

plots corresponds to the time window defined for the current study, where the same distance between the input and sensor has been used for all the tests.

The results show how by applying the method described in section 6 it is possible to obtain an index associated with the cumulative value of the standard deviation that defines the status of the tensioning forces. The index value can be observed to be increasing when the tensioning forces in the contact wire drop, allowing the detection of changes from the nominal force conditions. The trend appears to be the same in the results from the analytical formulation, where the method was built, as well as in the results from the measured accelerations, where the method was tested and showed consistency.

From Figure 10a, an observation can be made regarding the effects on the index due to the variation in the wire cross-section. It can be noted how both the CW100-7.06 kN and CW080-6.98 kN have the same value of cumulative standard deviation, as if the tension, more than the cross-section, is what influences the index value to a greater extent. However, looking at the results from the measured data, it also looks like the reduction in cross-section influences the index. A possible explanation for this small discrepancy can be found in the difference between the laboratory test setup, the field measurements, and their equivalent analytical models. The analytical models represent, in both cases, a perfect system, with total reflection at the ends and partial reflection at the dropper clamps. On the other hand, the behaviour of the wires from laboratory tests and field measurements is influenced by the presence of uncertainties that cannot be taken into consideration by the analytical model, such as friction in the end clamps in the pulling machine used in the laboratory or a tensioning force not in accordance with the nominal value for the field measurements.

Nevertheless, the behaviour of the index trend associated with the change in tension does not show inconsistency despite the uncertainties. This aspect is of high relevance when it comes to applying the method, as it has proven to be robust enough to overcome the differences in configuration and environmental background, returning reliable information on the change in the wire tension value.

8. Conclusions

The work presented in this paper shows a successful method developed for monitoring the behaviour of the tensioning forces applied to contact wires in railway catenary systems. Infrastructure monitoring has gained considerable attention in recent years, requiring easy and fast techniques for the detection of system degradation. Following this scope, the evaluation of the cumulative standard deviation on the contact wire vertical accelerations was used as an index of tensioning force variation over time. The accelerations needed for this method were identified in the vertical accelerations caused by the waves propagating along the contact wire when a train is running under the corresponding catenary section. The procedure includes the sensor positioning, the time window choice for the analysis, and the evaluation of the cumulative standard deviation of the acceleration signal. The method was built and refined by analysing the vertical acceleration values obtained from a novel analytical formulation of the propagation of waves in a tensioned wire. Afterwards, the method was tested on acceleration values coming from laboratory tests and field measurements, and the results were compared.

A consistent trend was found where the index value, namely, the cumulative value for the moving standard deviation, increases with the decrease of the tensioning forces. In this way, an evaluation of this index at each train passage would be able to detect an eventual drift from the nominal value of the contact wire tensioning forces and trigger a maintenance intervention when needed.

Acknowledgements

The authors are grateful to the Norwegian Railway Directorate, Bane NOR and Spordrift for their assistance with field measurements.

Declaration of conflicting interests

The authors declare no potential conflicts of interest with respect to the research, authorship, and/or publication of this article.

Funding acknowledgements

The authors disclosed receipt of the following financial support for the research, authorship, and/or publication of this article: this work was supported by the Norwegian Railway Directorate.

References

1. Gostling RJ, Hobbs AEW. The Interaction of Pantograph and Overhead Equipment: Practical Applications of a New Theoretical Method. *Proc Inst Mech Eng Part C J Mech Eng Sci* 1983; 197: 61–69.

2. Bruni S, Bucca G, Carnevale M, et al. Pantograph–catenary interaction: recent achievements and future research challenges. *Int J Rail Transp* 2017; 00: 1–26.

3. Bruni S, Ambrosio J, Carnicero A, et al. The results of the pantograph-catenary interaction benchmark. *Veh Syst Dyn* 2015; 53: 412–435.

4. Rønnquist A, Nåvik P. Dynamic assessment of existing soft catenary systems using modal analysis to explore higher train velocities: A case study of a Norwegian contact line system. *Veh Syst Dyn* 2015; 53: 756–774.

5. Anastasio D, Fasana A, Garibaldi L, et al. Analytical investigation of railway overhead contact wire dynamics and comparison with experimental results. *Mech Syst Signal Process* 2019;

116: 277–292.

6. Nåvik P, Rønnquist A, Stichel S. The use of dynamic response to evaluate and improve the optimization of existing soft railway catenary systems for higher speeds. *Proc Inst Mech Eng Part F J Rail Rapid Transit* 2015; 230: 1388–1396.

7. Gregori S, Tur M, Nadal E, et al. An approach to geometric optimisation of railway catenaries. *Veh Syst Dyn* 2018; 56: 1162–1186.

8. Nåvik P, Rønnquist A, Stichel S. Identification of system damping in railway catenary wire systems from full-scale measurements. *Eng Struct* 2016; 113: 71–78.

9. Zou D, Zhang WH, Li RP, et al. Determining damping characteristics of railway-overhead-wire system for finite-element analysis. *Veh Syst Dyn* 2016; 54: 902–917.

10. Ikeda K. Optimization of Overhead Contact Lines for Shinkansen Speed Increases. *JR EAST Tech Rev* 2008; 64–69.

11. Bruni S, Bucca G, Collina A, et al. Numerical and Hardware-In-the-Loop Tools for the Design of Very High Speed Pantograph-Catenary Systems. *J Comput Nonlinear Dyn* 2012; 7: 041013.

12. Facchinetti A, Bruni S. Hardware-in-the-loop hybrid simulation of pantographcatenary interaction. *J Sound Vib* 2012; 331: 2783–2797.

13. Kiessling F, Puschmann R, Schmieder A, et al. *Contact Lines for Electric Railways*. 3rd ed. Erlangen: Publicis, 2018.

14. Aboshi M, Manabe K. Analyses of contact force fluctuation between catenary and pantograph. *Q Rep RTRI (railw Tech Res Institute)* 2000; 41: 182–187.

15. Hayasaka T. Effect of reduced reflective wave propagation on overhead contact lines in

overlap section. *Q Rep RTRI (railw Tech Res Institute)* 2004; 45: 68–73.

16. Park SY, Jeon BU, Lee JM, et al. Measurement of Low-Frequency Wave Propagation in a Railway Contact Wire with Dispersive Characteristics Using Wavelet Transform. *Key Eng Mater* 2006; 321–323: 1609–1615.

17. Zou D, Zhou N, Rui Ping L, et al. Experimental and simulation study of wave motion upon railway overhead wire systems. *Proc Inst Mech Eng Part F J Rail Rapid Transit* 2017; 231: 934–944.

18. Vo Van O, Massat JP, Balmes E. Waves, modes and properties with a major impact on dynamic pantograph-catenary interaction. *J Sound Vib* 2017; 402: 51–69.

19. Sorrentino S, Anastasio D, Fasana A, et al. Distributed parameter and finite element models for wave propagation in railway contact lines. *J Sound Vib* 2017; 410: 1–18.

20. Song Y, Liu Z, Duan F, et al. Wave propagation analysis in high-speed railway catenary system subjected to a moving pantograph. *Appl Math Model* 2018; 59: 20–38.

21. Lanza di Scalea F, McNamara J. Measuring high-frequency wave propagation in railroad tracks by joint time-frequency analysis. *J Sound Vib* 2004; 273: 637–651.

22. Zumpano G, Meo M. A new damage detection technique based on wave propagation for rails. *Int J Solids Struct* 2006; 43: 1023–1046.

23. Nåvik P, Rønnquist A, Stichel S. A wireless railway catenary structural monitoring system: Full-scale case study. *Case Stud Struct Eng* 2016; 6: 22–30.

24. Diana G, Falco M, Fasciolo S, et al. Experimental and Numerical Investigation on the Dynamic Behaviour of the Catenary for AV Italian Railway Line. In: *WCRR '97, Florence, November 16-19*. Florence, 1997, pp. 1–17.

25. Drugge L, Larsson T, Stensson A. Modelling and simulation of catenary-pantograph interaction. *Veh Syst Dyn* 2000; 33: 490–501.

26. Stickland MT, Scanlon TJ, Craighead IA, et al. An investigation into the mechanical damping characteristics of catenary contact wires and their effect on aerodynamic galloping instability. *Proc Inst Mech Eng Part F J Rail Rapid Transit* 2003; 217: 63–71.

27. Metrikine A V., Bosch AL. Dynamic response of a two-level catenary to a moving load. *J Sound Vib* 2006; 292: 676–693.

28. Dahlberg T. Moving force on an axially loaded beam—with applications to a railway overhead contact wire. *Veh Syst Dyn* 2006; 44: 631–644.

29. Cho YH. Numerical simulation of the dynamic responses of railway overhead contact lines to a moving pantograph, considering a nonlinear dropper. *J Sound Vib* 2008; 315: 433–454.

30. Facchinetti A, Gasparetto L, Bruni S. Real-time catenary models for the hardware-in-The-loop simulation of the pantograph-catenary interaction. *Veh Syst Dyn* 2013; 51: 499–516.

31. Gregori S, Tur M, Pedrosa A, et al. A modal coordinate catenary model for the real-time simulation of the pantograph-catenary dynamic interaction. *Finite Elem Anal Des* 2019; 162: 1–12.

32. Rønnquist A. *Pedestrian induced lateral vibrations of slender footbridges*. 2005.

33. NEK EN 50149:2012 Railway applications - Fixed installations - Electric traction - Copper and copper alloy grooved contact wires.